Parasite Immunology, 2008, **30**, 497–514 DOI: 10.1111/j.1365-3024.2008.01050.x

Blood stage malaria antigens induce different activation-induced cell death programs in splenic CD4$^+$ T cells

P. MUKHERJEE, Y. S. DEVI & V. S. CHAUHAN

International Centre of Genetic Engineering and Biotechnology, Aruna Asaf Ali Road, New Delhi, India

SUMMARY

CD4$^+$ T cells respond to antigen immunization through a process of activation, clonal expansion to generate activated effector T cells followed by activation-induced clonal deletion of the responding T cells. While loss of responding T cells in post-activation death by apoptosis is a major factor regulating immune homeostasis, the precise pathways involved in down-sizing of Plasmodium falciparum *antigen-induced T cell expansions are not well characterized. We report in this study that splenic CD4$^+$ T cells from mice immunized with non-replicating immunogens like OVA or recombinant blood stage* P. falciparum *antigens, PfMSP-3 and PfMSP-1$_{19}$ or crude parasite antigen (PfAg) undergo sequential T cell activation, proliferation followed by activation-induced cell death (AICD) in a dose- and time-dependent manner after Ag restimulation. While PfMSP-3 and OVA-induced AICD was mediated through a death receptor-dependent apoptotic program, PfMSP-1$_{19}$ and PfAg-induced AICD was via a mechanism dependent on the activation of mitochondria apoptosis signalling pathway through Bax activation. These results provide insights into the mechanism through which two blood stage merozoite antigens trigger different apoptotic programs of AICD in splenic CD4$^+$ T cells.*

Keywords *AICD, CD4$^+$ T cells, death receptor pathway, mitochondrial death pathway,* P. falciparum *recombinant antigen*

INTRODUCTION

CD4$^+$ T cells respond to foreign antigen by becoming activated proliferating effector cells and after clonal expansion, majority of the effector cells die by apoptosis. Apoptotic cell death is an important mechanism for maintaining homeostasis in the T cell compartment and regulating the fates of T cells following encounters with foreign antigens. The majority of activated T cells undergo activation-induced cell death (AICD), in which activation through the TCR with antigen or polyclonal activators (e.g. superantigens) results in apoptosis (1). CD4$^+$ T cell death is also determined by a number of factors such as the nature and intensity of TCR signalling, lack of costimulation, the availability of cytokines or aberration in the cell cycle program (1–4).

Several studies have revealed two major apoptotic pathways, the extrinsic death receptor pathway and the intrinsic mitochondrial pathway that control apoptosis of CD4$^+$ T cell (4,5). Ligation of death receptors (such as Fas, TNFR1, DR3, DR4 and DR5) with their respective ligands convey apoptotic signals to adaptor molecules that recruit and activate a family of cysteine proteases, caspases. Activation of caspases lead to a cascade of molecular events that result in biochemical as well as morphologic alterations associated with programmed cell death (6–10). In the second death pathway, mitochondrial dysfunction plays a central role in commitment of cells to apoptosis (11). The mitochondrial death pathway is characterized by a decrease in mitochondrial transmembrane potential, release of apoptogenic proteins such as cytochrome c and apoptosis-inducing factor (AIF) and the activation of caspases (12). Members of the Bcl-2 family of proteins regulate the changes in the mitochondrial membrane permeability and in the release of apoptogenic factors (13,14).

Immunity to asexual blood stage malaria is dependent on both humoral as well as cellular immune responses (15–17). Recent studies suggest that malaria parasites may actually modulate or even exploit the host immune responses to facilitate its survival in an antagonistic environment (18–20). Cellular immune responses may be initiated against merozoites antigens subsequent to phagocytosis and processing of infected red

Correspondence: Paushali Mukherjee, Virander S. Chauhan, International Centre of Genetic Engineering and Biotechnology, Aruna Asaf Ali Road, New Delhi 110067, India
(e-mails: paushali@icgeb.res.in; virander@icgeb.res.in).
Received: 9 October 2007
Accepted for publication: 26 May 2008

blood cells, free merozoites or cellular debris. $CD4^+$ T cells dictate the quality and the fate of the protective immune responses to asexual blood stage malaria in both human as well as murine models (21–23). The acute malaria infection is associated with defects in cellular immune responses that have been attributed to alterations in the T cell functions. *Plasmodium* parasite may have developed apoptosis of T cells as an evasive mechanism to suppress the efficiency of host's immune system to control infection. Some studies have shown that PBL obtained from patients during acute blood stage infection fails to respond to antigens derived from malaria parasites or to mitogen while others have shown that there were no differences in the response to mitogenic stimulation of PBMC from infected patients and controls (24–28). Also, during malaria infection a proportion of the lymphocyte population were found to be sensitive to apoptosis but only after an interval of time before *in vivo* activated cells would express the apoptotic process *in vitro* (28–31). Apoptosis was found to be significantly increased in the CD4 T cell subset compared to CD8 and γδ T cells in *Plasmodium falciparum* infected patients and contributed to the low frequency and number of $CD4^+$ T cells in the peripheral circulation during active disease (32,33).

The blood stage merozoites express a number of surface antigens that are involved in the initial interaction between the parasite and the host erythrocytes (34). These antigens act both as targets for the immune response and as negative regulators of host immunity (35). Merozoite surface protein-1 (MSP-1) and MSP-3 are both involved in the development of protective humoral immunity against malaria infection. MSP-1 undergoes a series of proteolytic cleavages resulting in the highly conserved 19 kDa carboxy-terminal fragment, PfMSP-1_{19}, which is associated with the merozoite during the invasion (36,37). Several studies have provided evidences suggesting that the MSP-1_{19} is the target of protective immunity against asexual blood stages of malaria parasites (36,37). MSP-3 is a 48-kDa molecule of unknown function associated with the merozoite surface (38,39). MSP3-specific cytophilic antibodies are effective in controlling parasite multiplication by the antibody-dependent cellular inhibition mechanism (39,40). Recent murine malaria models have shown that the parasite-specific as well as 19-kDa carboxyl-terminal fragment of *P. yoelli* MSP-1 (PyMSP-1_{19}-specific $CD4^+$ T cells) were depleted after infection with both lethal and nonlethal species of rodent *Plasmodium* and this deletion significantly affected the protective immunity to malaria (41,42). However, still remaining unclear is the pathway(s) through which the parasite or parasite-antigen induces apoptosis of $CD4^+$ T cells during blood stage malaria infection. Identifying the molecular mechanisms involved in the apoptosis of $CD4^+$ T cells would be relevant to understanding of the malaria immunity and, in particular, to malaria vaccine research.

In this study we sought to determine the fate of $CD4^+$ T cells in mice immunized with increasing doses of two recombinant MSPs, PfMSP-1_{19} and PfMSP-3 and crude *P. falciparum* antigen (PfAg). We found that PfMSP-1_{19} and PfMSP-3 as well as PfAg sensitize mouse splenic $CD4^+$ T cells sequentially to activation, proliferation followed by AICD through distinct apoptotic program. Our study demonstrates that apoptosis induced in $CD4^+$ T cells by PfMSP-3 is Fas mediated and involved activation of caspase-8 and -3 whereas PfMSP-1_{19} and PfAg enhanced AICD via a mechanism dependent on the activation of mitochondrial apoptosis signalling pathway involving changes in Bcl-2 : Bax ratio and the release of cytochrome c and activation of caspase-9.

MATERIALS AND METHODS

Mice

Female BALB/c ($H\text{-}2^d$) mice aged 8–10 weeks were purchased from The Jackson Laboratory (Bar Harbor, ME) and maintained in the pathogen-free small animal facility of the International Centre of Genetic Engineering and Biotechnology (New Delhi, India). All animal experimentations were done in accordance to the protocols approved by the Institutional Animal Ethics Committee (IAEC).

Antigens

Gene for PfMSP-3 full protein (PfMSP-3) and synthetic gene for 19 kDa fragment of PfMSP-1 designed based on codon bistable of *Escherichia coli*, were cloned into the expression vector pET28a(+) (Novagene) and transformed into *E. coli* BLR (DE3) host cells. Expression of the recombinant PfMSP-3 and PfMSP-1_{19} were induced with 1 mM isopropyl-β-D-thiogalactopyranoside (IPTG) (Sigma-Aldrich, St. Louis, MO). For the purification of PfMSP-3 and PfMSP-1_{19} proteins, the induced pellets were sonicated and the recombinant protein present in the soluble fraction was purified by metal affinity chromatography using nickel–NTA-matrix (Qiagen, Valencia, CA). Purified recombinant PfMSP-3 and PfMSP-1_{19} were analysed for purity and homogeneity by sodium dodecyl sulphate (SDS)–polyacrylamide gel electrophoresis (PAGE) and reverse-phase chromatography. Mass spectrum analysis and N-terminal sequencing confirmed the molecular identity of the purified PfMSP-3 and PfMSP-1_{19}. The protein preparations contained < 2 endotoxin units per mg of protein. To prepare crude parasite antigen (PfAg), mature schizonts of *P. falciparum* parasites of the 3D7 strain were harvested from synchronized cultures of 10% parasitaemia by centrifugation through 60% Percoll gradients (Sigma). Schizont-infected erythrocytes were washed three times in serum-free medium to remove endogenous serum proteases

and other proteins. The parasites (10^8/mL) were lysed with 0·01% saponin/PBS at 4°C for 10 min followed by sonication in the presence of protease inhibitors (Sigma). After sonication, the lysate was centrifuged at 14 000 ***g*** for 30 min at 4°C. The protein concentration was determined by bicinchoninic acid (BCA) assay (Pierce, Rockford, IL). As nonmalaria antigen, ovalbumin (OVA) (Sigma) was used.

Immunizations

A total of 6–8 BALB/c mice per group were treated subcutaneously with phosphate buffered saline (PBS), or 25, 50 or 100 μg of recombinant MSP-1_{19}, PfMSP-3F, PfAg or OVA in CFA and boosted 2 weeks later with same amount of antigen in IFA. 7 days after boosting, splenic CD4+ T cells were purified from these mice and used as primed cells. Splenic CD4+ T cells from adjuvant control mice were used as unprimed cells.

Purification of CD4+ T cells and antigen-presenting cells (APCs) from spleen and stimulation

Unprimed and antigen primed CD4+ T cells were purified from spleens with the MACS CD4 Multisort Kit (Miltenyi Biotech, Auburn, CA). The purity of the CD4 cells (95–98%) was confirmed by flow cytometric analysis using anti-CD4 antibodies (BD PharMingen, San Diego, CA). APCs were purified using anti-MHC II beads (MACS, Miltenyi Biotech) from spleens of naive syngenic mice. In total, 5×10^5 purified CD4+ T cells from primed mice were cultured with medium alone, or titrated dose of PfMSP-1_{19}, PfMSP-3, PfAg or anti-CD3e antibodies in the presence of 1×10^6 splenic APCs at 37°C in a 5% CO_2 atmosphere for 24–96 h in RPMI-1640 (Invitrogen Life Technologies, Grand Island, NY) supplemented with 10% fetal bovine serum (Invitrogen), 2 mM glutamine, 10 mM HEPES, 50 μM 2-ME, 0·1 mg/mL streptomycin and 100 U/mL penicillin. Cells were pulsed with 1·0 μCi/well of [^{3}H]thymidine during the last 16 h of culture and labelled cells were harvested and counted by liquid scintillation (Betaplate; Wallac, Turku, Finland). Data are expressed as mean counts per minute (cpm) of triplicate cultures. SEM was < 20% of the mean values.

To delineate the AICD pathway, activated CD4+ T cells were pretreated with 10 μg/mL of various soluble decoy proteins such as human Fas–Fc immunoglobulin fusion protein (binds CD95L and blocks the receptor-ligand interaction), TNFR.Fc (binds TNF and blocks the receptor-ligand interaction), TRAIL.Fc (binds TRAIL and blocks the receptor–ligand interaction), or 50 μM of pan specific caspase inhibitor, caspase-3 inhibitor, caspase-8 inhibitor and caspase-9 inhibitor (all from R&D Systems Inc., Minneapolis, MN) for 1 h. Caspase inhibitors were dissolved in DMSO and control cultures were performed in the presence of diluted DMSO, dilution not exceeding 0·1%. Cells were then stimulated with recall antigen and splenic APCs in the absence or presence of soluble decoy proteins or different caspase inhibitors for 72 h, and thereafter CD4 T cell death was measured.

Flow cytometry analysis of apoptotic cells and expression of apoptotic regulatory markers

Apoptosis was measured by three-colour flow cytometry. A total of 1×10^6 splenocytes were stained with cychrome-conjugated CD4 and PE conjugated CD44 for 30 min on ice. Cells were washed with PBS and stained with FITC labelled annexin V (BD PharMingen). After incubation for 15 min at room temperature in the dark cells were immediately analysed on a FACSCaliber flow cytometer (BD Immunocytometry System, San Jose, CA). For the detection of T cells activation markers and expression of apoptotic regulatory molecules, cells were stained with indicated Abs in PBS supplemented with 1% FCS and 0·1% sodium azide for 30 min on ice. Cells were then washed and analysed on a BD Biosciences FACSCalibur. The following conjugated Abs (from BD Pharmingen) were used for flow cytometric analyses: anti-CD4 PE, anti-CD4 Cychrome, anti-CD44 PE, anti-CD62L FITC, anti-CD69 FITC, anti-CD25 PE anti-CD45RB FITC, anti-Fas PE, anti-FasL PE. For intracellular staining for Bcl-2 family members, cells were surface stained as described above, fixed with 1% paraformaldehyde for 30 min, washed twice in permeabilization buffer (PBS with 0·3% saponin, 1% FCS, and 0·1% sodium azide) fixed with 1% paraformaldehyde and then stained with either hamster anti-Bcl-2 mAb (PharMingen) or rabbit anti-Bax Ab (R&D System), followed by either FITC-labelled goat antihamster IgG Ab (eBioscience, San Diego, CA) or goat antirabbit IgG Ab (Sigma) diluted in permeabilization buffer and all incubations were of 40-min duration on ice. Isotype matched FITC/PE tagged controls (eBioscience) were included with each set. Cells were resuspended in saponin-free buffer. At least 30 000 cells were acquired on a BD FACSCalibur flow cytometer (BD Biosciences) and the data was analysed with FlowJo software (Treestar, San Jose, CA).

Preparation of cell lysates and subcellular fractionation

Stimulated CD4+ T cells (2×10^6 cells) were washed twice with chilled PBS and lysed by suspending the cells in 50 μL of Triton X-100 lysis buffer (30 mM Tris–HCl, pH7·5, 150 mM NaCl, 2 mM EDTA, 1 mM PMSF and 10 μg/mL of peptide inhibitors leupeptin, pepstatin, aprotinin 1% Triton X-100 and 10% glycerol on ice for 30 min, followed by centrifugation at 14 000 ***g*** at 4°C for 15 min. The subcellular fractionation of CD4+ T cells was according to the published protocol (32). Simulated CD4+ T cells (2×10^6 cells) were washed twice with ice-cold PBS and resuspended in 100 μL digitonin lysis buffer containing 190 μg/mL of digitonin,

Journal compilation © 2008 Blackwell Publishing Ltd, *Parasite Immunology*, **30**, 497–514

250 mM sucrose, 8 mM Na_2HPO_4, 1 mM NaH_2PO4 75 mM NaCl, 1 mM PMSF, and 10 μg/mL of protease inhibitors aprotitin, pepstatin, and leupeptin. After 5 min incubation at 4°C, cells were centrifuged at 14 000 *g* for 5 min at 4°C. The resulting supernatant was transferred to a fresh tube designated as cytosol. The pellet was resuspended in 0·1% Triton X-100 lysis buffer (25 mM Tris–HCl buffer (pH 8·0), 0·1% Triton X-100) and designated as mitochondrial fraction. Protein concentration in the cell lyaste and subcellular fractions were measured by bicinchoninic acid (Pierce) protein assay.

Western blotting

For Western blot detection of proteins, cell lysates or subcellular fractions equivalent to 2×10^6 cells were boiled for 5 min in 50 μL of 2 × Laemmli buffer. A measure of 20 μL of the samples were resolved (2×10^6/lane) on 10%, 12% or 15% SDS-PAGE gels depending on the protein being detected. After electrophoresis proteins were transferred to Hybond nitrocellulose membrane (Amersham Bioscience, Piscataway, NJ) and blocked with 5% milk in phosphate-buffered saline with 0·05% Tween-20 (Sigma) overnight at 4°C. Membranes were washed with PBS/Tween and then incubated with anti-Bax and anti-cytochrome c (from PharMingen). The blots were washed with PBS/Tween and developed with horseradish-peroxidase conjugated secondary antibodies in 0·1% milk PBS/Tween. Western blots were developed using enhance chemiluminescence kit (Amersham Bioscience).

Caspase colourimetric assay

Antigen primed $CD4^+$ T cells were not treated or pretreated with 10 μg/mL of various soluble decoy proteins such as human Fas–Fc immunoglobulin fusion protein or 50 μM of caspase-3 inhibitor, caspase-8 inhibitor and caspase-9 inhibitor. Cells were then stimulated with recall antigen and splenic APCs in the absence or presence of Fas-Fc or different caspase inhibitors for 96 h, and thereafter caspase-8, caspase9 and caspase-3 activity was measured by a colourimetric assay according to the manufacturer's instructions (R&D System). Briefly, 2×10^6 cells were lysed and the lysate was tested for cleavage of IETD-pNA, LEDH-pNA and DEVD-pNA, substrate for caspase-8, caspase9 and caspase-3, respectively, and the results were expressed as absorbance at 405 nm.

Statistics

Statistical significance was calculated by a 2-sample 2-tailed Student's *t*-test (GraphPad InStat). Comparisons were considered statistically significant at $P < 0{\cdot}05$.

RESULTS

Proliferative response of PfMSP-1_{19} or PfMSP-3 primed $CD4^+$ T cells

In the present study we examined the effects of recombinant *P. falciparum* antigens on proliferation, clonal expansion, and apoptosis of splenic $CD4^+$ T cells *in vitro*. In initial experiments, mice were immunized with increasing dose (25, 50 or 100 μg) of PfMSP-1_{19}, PfMSP-3 or crude PfAg and OVA (OVA was used as nonmalarial antigen) twice in CFA/IFA and 7 days after the last immunization, splenic $CD4^+$ T cells were stimulated *in vitro* with various doses of recall antigen plus APCs. *Ex vivo* $CD4^+$ T cells from mice immunized with 25, 50 or 100 μg of PfMSP-1_{19} PfMSP-3, PfAg or OVA revealed a highly activated phenotype with up-regulated levels of CD25, CD44 and CD69 expression and reduced levels of CD62L and CD45RB compared to adjuvant control mice (Table 1). However, irrespective of the antigen dose, $CD4^+$ T cells from immunized mice showed heterogeneous proliferative responses to recall antigen or anti-CD3. $CD4^+$ T cells from mice immunized with 25, 50 or 100 μg of PfMSP-1_{19} demonstrated considerably decreased proliferative responses when stimulated with titrated dose of recall antigen or anti-CD3 (Figure 1a). Similar results were obtained with splenic $CD4^+$ T cells from mice primed with PfAg (Figure 1a). In contrast, the proliferative responses of $CD4^+$ T cells from PfMSP-3 or OVA immune mice increased with increasing Ag doses administered to mice (25, 50 or 100 μg), but the increased response seen after high dose PfMSP-3 was not significant ($P = 0{\cdot}21$) (Figure 1a). In case of OVA, high dose (100 μg) showed significant increase in the proliferative response compared to 25 μg ($P < 0{\cdot}05$) (Figure 1a). $CD4^+$ T cells purified from various antigen primed mice failed to respond to heterologous antigen stimulation (data not shown). $CD4^+$ T cells purified from adjuvant control mice proliferated in response to anti-CD3 stimulation but not in response to malaria antigens or OVA (Figure 2a). Further, in the absence of splenic APCs, antigen-primed $CD4^+$ T cells showed no proliferative response to recall antigen even at high antigen dose (Figure 2b), indicating that recombinant malaria antigens did not have mitogenic effect on $CD4^+$ T cells and that accessory cells are essential for the induction of T-cell proliferation.

Comparing the proliferative response between various antigen primed $CD4^+$ T cells, PfMSP-3 primed $CD4^+$ T cells showed enhanced proliferation compared with PfMSP-1_{19}- or PfAg-primed $CD4^+$ T cells after stimulation with anti-CD3 irrespective of the priming dose (Figure 2c). However, $CD4^+$ T cells from OVA-primed mice showed significant proliferation in response to anti-CD3 stimulation compared to PfMSP-3 primed $CD4^+$ T cells ($P < 0{\cdot}01$) and PfMSP-1_{19}-

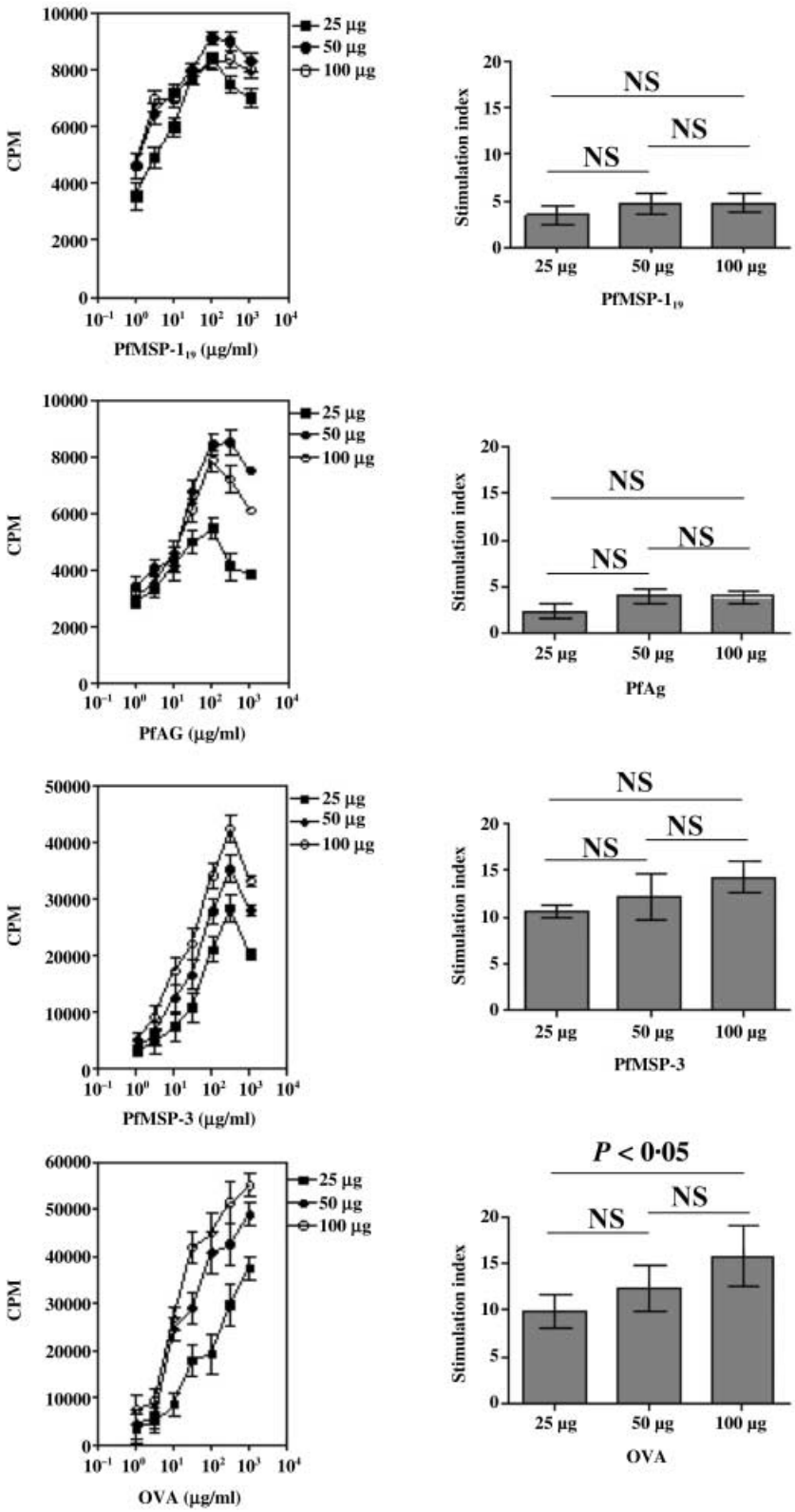

Figure 1 Proliferative activity of CD4+ T cells from mice primed with PfMSP-1_{19} and PfMSP-3. Mice were administered twice with increasing dose of recombinant PfMSP-1_{19}, PfMSP-3, crude *P. falciparum* antigen (PfAg), control antigen OVA (25, 50 and 100 µg per mouse) or PBS in CFA/IFA. Cultures were set up 7 days after last immunization. Proliferative responses of purified CD4+ T cells from the spleen of the immune mice in the presence of syngenic splenic APCs are represented as counts per minute of [^{3}H]thymidine incorporation in triplicate cultures in response to titrating doses of recall antigen *in vitro* (left panels) and as the stimulation index determined by dividing the mean experimental proliferation value by the mean of the medium control proliferation value at a representative (100 µg/mL) dose of recall antigen (right panels). Background levels of [^{3}H]thymidine incorporation in the absence of antigenic stimulation were 1250–2500 cpm. The results are representative of three experiments. Statistical significance for each group is indicated above the bars. NS, not significant.

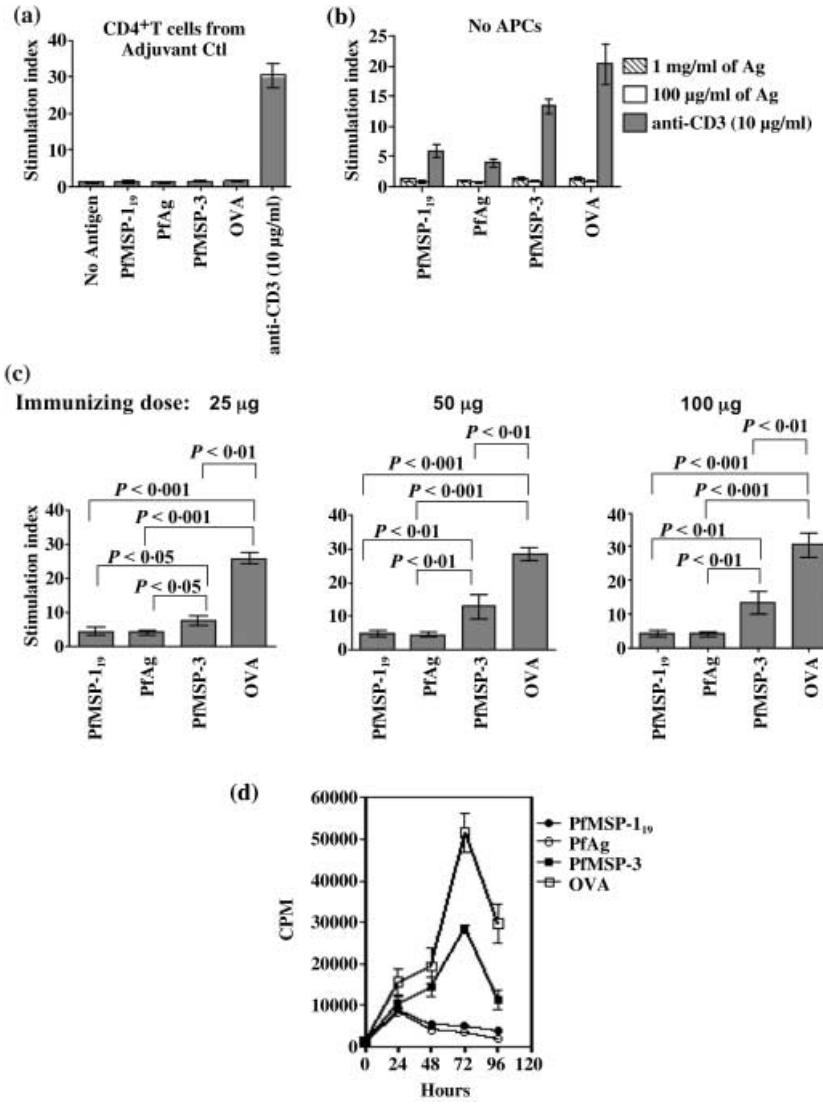

Figure 2 Proliferative activity of CD4$^+$ T cells from adjuvant control mice or antigen primed mice following antigen or polyclonal stimulation. Mice were administered twice with increasing dose of recombinant PfMSP-1$_{19}$, PfMSP-3, crude *P. falciparum* antigen (PfAg), control antigen OVA (25, 50 and 100 µg per mouse) or PBS in CFA/IFA. Cultures were set up 7 days after last immunization. (a) Proliferative responses of purified CD4$^+$ T cells from the spleen of the adjuvant control mice in the presence of syngenic splenic APCs in response to (100 µg/mL) dose of recall antigen. The proliferative responses are given as a stimulation index determined by dividing the mean experimental proliferation value by the mean of the medium control proliferation value. (b) Proliferative responses of purified CD4$^+$ T cells from the spleen of the antigen primed mice in the absence of syngenic splenic APCs in response to two doses of recall antigen (1 and 100 µg/mL) and10 µg/mL of anti-CD3 antibodies. The proliferation values are given as a stimulation index determined by dividing the mean experimental proliferation value by the mean of the medium control proliferation value. (c) Proliferative responses of purified CD4$^+$ T cells from the spleen of mice primed with increasing dose of antigen in the presence of splenic APCs in response to 1 µg/mL of anti-CD3 antibodies. The proliferative responses are given as a stimulation index determined by dividing the mean experimental proliferation value by the mean of the medium control proliferation value. Data are representative of those from three experiments. Statistical significance for each group is indicated above the bars. (d) Purified CD4$^+$ T cells from the spleen of mice primed with 50 µg antigen were stimulated with 100 µg/mL of recall antigen in the presence of syngenic splenic APCS and T cell proliferation was assayed at the times indicated. Data are represented as mean ± SE of counts per minute and are representative of two independent experiments.

Table 1 Activation phenotype of *ex vivo* CD4+ T cells from mice immunized with different doses of PfMSP-1_{19}, PfAg, PfMSP-3 and OVA[a]

	PfMSP-1_{19}			PfMSP-3			PfAg			OVA		
Adjuvant control	25 µg	50 µg	100 µg	25 µg	50 µg	100 µg	25 µg	50 µg	100 µg	25 µg	50 µg	100 µg
CD25	12 ± 1%	50 ± 9%	79 ± 10%	80 ± 12%	74 ± 8%	85 ± 7%	92 ± 13%	66 ± 10%	77 ± 9%	72 ± 11%	64 ± 4%	87 ± 13%	92 ± 14%
	(14 ± 0.9)	(17 ± 2)	(24 ± 2)	(25 ± 6)	(25 ± 7)	(45 ± 8)	(46 ± 8)	(25 ± 6)	(30 ± 3)	(31 ± 7)	(35 ± 8)	(40 ± 4)	(47 ± 7)
CD45RB	76 ± 9%	28 ± 6%	18 ± 1%	17 ± 1%	22 ± 3%	13 ± 1%	11 ± 2%	39 ± 5%	14 ± 2%	13 ± 2%	17 ± 1%	11 ± 3%	9 ± 2%
	(196 ± 9)	(187 ± 21)	(163 ± 29)	(15 ± 22)	(154 ± 37)	(136 ± 19)	(131 ± 11)	(157 ± 2)	(144 ± 7)	(140 ± 38)	(132 ± 12)	(196 ± 9)	(196 ± 9)
CD62L	78 ± 14%	25 ± 9%	9 ± 2%	10 ± 3%	16 ± 2%	7 ± 0.3%	7 ± 1%	33 ± 4%	19 ± 0.9%	18 ± 3%	14 ± 2%	6 ± 0.9%	6 ± 1%
	(50 ± 9)	(42 ± 4)	(36 ± 3)	(34 ± 5)	(40 ± 1)	(30 ± 6)	(29 ± 3)	(44 ± 4)	(38 ± 4)	(35 ± 4)	(40 ± 4)	(27 ± 4)	(24 ± 4)
CD69	16 ± 2%	43 ± 9%	61 ± 11%	62 ± 13%	54 ± 12%	71 ± 17%	74 ± 14%	31 ± 6%	59 ± 5%	58 ± 8%	66 ± 10%	68 ± 11%	65 ± 11%
	(14 ± 1)	(17 ± 4)	(27 ± 3)	(29 ± 4)	(25 ± 1)	(47 ± 1)	(47 ± 10)	(17 ± 2)	(25 ± 1)	(25 ± 1)	(25 ± 1)	(54 ± 1)	(56 ± 1)
CD44	19 ± 3%	81 ± 16%	92 ± 14%	94 ± 18%	89 ± 21%	99 ± 23%	99 ± 24%	73 ± 20%	82 ± 18%	85 ± 19%	92 ± 21%	99 ± 23%	99 ± 20%
	(281 ± 20)	(281 ± 20)	(589 ± 40)	(587 ± 80)	(438 ± 29)	(781 ± 95)	(788 ± 61)	(277 ± 34)	(490 ± 70)	(491 ± 65)	(520 ± 49)	(811 ± 93)	(824 ± 120)

Mice were administered twice with increasing dose of recombinant PfMAP-1_{19}, PfMSP-3, crude *P. falciparum* antigen (PfAg), control antigen OVA (25, 50 and 100 µg per mouse) or PBS in CFA/IFA. 7 days after last immunization, splenic cells from Ag primed mice as well as from control adjuvant control mice were stained with anti-CD4 vs anti-CD25, anti-CD62L, anti-CD69 and anti-CD44.

[a]Both the percentage of cells and MF1 (given in brackets) are presented for each marker as mean ± SD.

or PfAg-primed CD4+ T cells ($P < 0{\cdot}001$) (Figure 2c). Furthermore, the reduced proliferation observed in PfMSP-1_{19}- or PfAg-primed CD4+ T cells was not due to a higher activation threshold because high concentrations of anti-CD3 stimulation (1 µg/mL) did not restore the impairment in proliferation in PfMSP-1_{19}- or PfAg-primed CD4+ T cells (Figure 2a).

Time-kinetic analysis of mice immunized with 50 µg of antigen further provided evidence that up to 24 h there was comparable proliferation of PfMSP-1_{19}, PfAg and PfMSP-3-primed CD4+ T cells, but significantly increased proliferation was evident by 72 h of PfMSP-3- and also OVA-primed CD4+ T cells (Figure 2d). Noticeably, proliferation in PfMSP-1_{19}-primed as well as PfAg-primed CD4+ T cell declined more rapidly than PfMSP-3-and OVA-primed CD4+ T cells, reaching baseline levels by 96 h after stimulation (Figure 3a). After 96 h of *in vitro* culture, CD4+ T cells from PfMSP-3 or OVA primed mice also displayed notable reduction in proliferative responses (Figure 2d). Irrespective of their proliferative response, PfMSP-1_{19}, PfMSP-3, PfAg or OVA-primed CD4+ T cells after recall stimulation induced a large population of activated CD4+ T cells and expressed surface markers characteristic of effector T cells: $CD4^{+}CD44^{high}$ $CD62L^{low}$ that was not evident in adjuvant control group (Figure 3).

Cell cycle progression in PfMSP-1_{19} and PfMSP-3 primed CD4+ T cells

Since activated PfMSP-1_{19} and PfAg-primed CD4+ T cells showed poor proliferating response following recall or anti-CD3 stimulation, we examined the expression of proliferation marker Ki-67, an indicator of cell cycle progression that is not expressed by the resting cells but increases in late G1 phase of the cell cycle indicating ongoing proliferation (43). A small proportion of *ex vivo* CD4+ T cells isolated from mice administered different doses of antigen expressed low but readily detectable levels of Ki-67, thus showing signs of active cell cycling at this time point (0 h) (Figure 4a). After 24 h of stimulation with recall antigen *in vitro*, there was a modest increase in the percentage of Ki-67 positive cells in PfMSP-1_{19} and PfAg primed CD4+ T cells indicating active cellular multiplication (Figure 4a). But after 48 h of stimulation, there was a progressive and marked decline in the percentage of Ki-67-positive cells (Figure 4a). These data indicate that the failure of PfMSP-1_{19} and PfAg-primed CD4+ T cells to proliferate in the presence of recall antigen results from a block in cell cycle progression. In contrast, in PfMSP-3 and OVA primed CD4+ T cells, there was an increase in the percentage of Ki-67 positive cells till 72 h of stimulation indicating that the cells were in active cell cycle phases. However, after 96 h of stimulation, percentage of

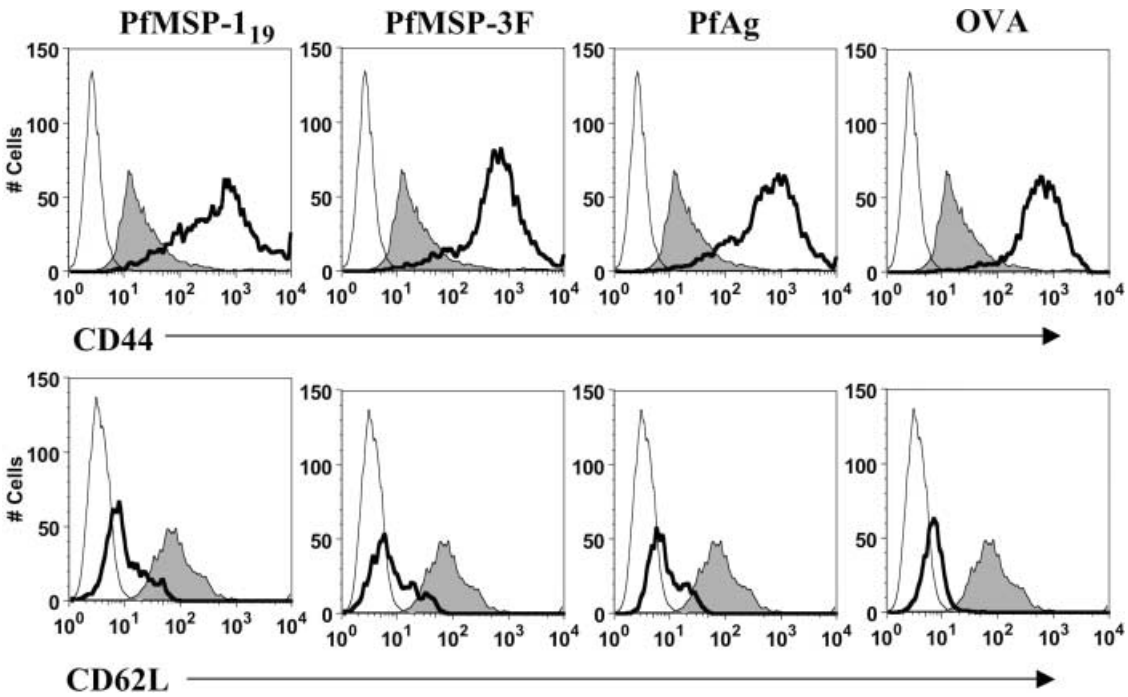

Figure 3 Activated phenotype of CD4$^+$ T cells from mice primed with PfSMP-1$_{19}$ and PfMSP-3. Purified CD4$^+$ T cells from the spleen of mice primed with 50 μg of PfMSP-1$_{19}$, PfAg, PfMSP-3, OVA or PBS in CFA/IFA were stimulated with 100 μg/mL of recall Ag in the presence of syngenic splenic APCS. 72 h after stimulation, cells were stained with anti-CD4 vs. anti-CD62L or anti-CD44 to detect activated phenotype. The CD62L and CD44 profiles of the gated CD4$^+$ T cells are shown as single-colour histograms. The grey thin line represent isotype control, grey filled histogram represent staining on cells from adjuvant control and thick black lines indicate staining on antigen stimulated cells. Data are representative of three independent experiments.

Ki-67 positive cells within PfMSP-3 and OVA-primed CD4$^+$ T cells decreased considerably marking the end of the proliferation phase (Figure 4a).

AICD of PfMSP-1$_{19}$ or PfMSP-3 primed CD4$^+$ T cells

We next determined whether the arrest of antigen-primed CD4$^+$ T cell proliferation observed following recall stimulation was due to increased T cell death. To address this issue, we determined the proportion of cells undergoing apoptosis in each of the activated antigen primed CD4$^+$ T cell by simultaneous annexin V, CD4 and CD44 staining. All four antigens used in the study (PfMSP-1$_{19}$, PfAg, PfMSP-3 and also OVA) induced cell death in antigen primed CD4$^+$ T cells in a time- and dose-dependent manner during *in vitro* stimulation with recall antigen (Figure 4b). The percentage of apoptotic cells in Ag primed CD4$^+$ T cells increased in a dose-dependent manner. PfAg and PfMSP-1$_{19}$ primed CD4$^+$ T cells showed maximal apoptotic cells (18% and 12%, respectively) at 100 μg/mL whereas PfMSP-3 and OVA primed CD4$^+$ T cells showed maximum annexin V$^+$ cells (7% and 6%, respectively) at 300–1000 μg/mL of recall antigen (Figure 4b). When purified CD4$^+$ T cells from mice primed with increasing antigen dose were co-cultured with APCs and recall antigen at 100 μg/mL, there was an increase in antigen-induced death with increasing priming dose from 25 to 50 μg ($P < 0{\cdot}05$), but there was no marked increase in apoptotic CD4$^+$ T cells when dose was increased from 50 to 100 μg in various antigen groups (Figure 4c). Culturing different antigen primed CD4$^+$ T cells with heterologous antigen plus APCs caused < 1% apoptosis in CD4$^+$ cells, indicating antigen specific response (data not shown). No AICD was induced in CD4$^+$ T cells isolated from adjuvant control mice when stimulated *in vitro* with PfMSP-1$_{19}$, PfMSP-3 or OVA indicating that these antigen preparations were not toxic to cells (Figure 4).

In time kinetic, at 24 h, the percentage of annexin V positive CD4$^+$ T cells was similar for PfMSP-1$_{19}$, PfAg and PfMSP-3 activated CD4$^+$ T cells (Figure 4c). However by 48 h, the PfMSP-1$_{19}$- and PfAg-activated CD4$^+$ T cells showed a greater percentage of annexin V positive cells that were more pronounced at 72 and 96 h compared to PfMSP-3-activated CD4$^+$ T cells (Figure 4c). It was also observed that compared to OVA-activated CD4$^+$ T cells, percentage of annexin V positive cells was higher amongst the malaria antigen primed CD4$^+$ T cells. These results suggest that the

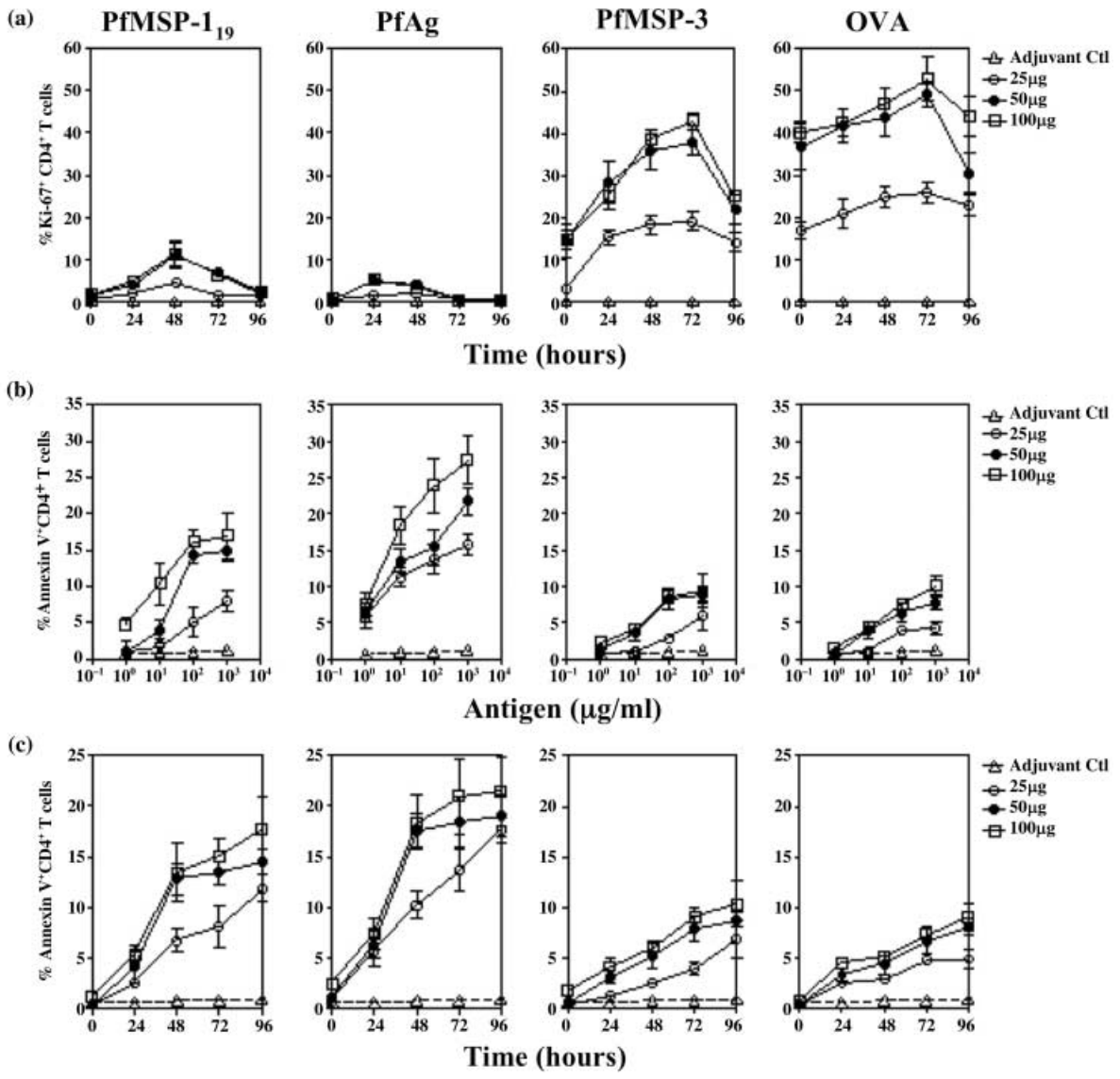

Figure 4 Cell cycle progression and activation-induced cell death of PfMSP-1_{19} and PfMSP-3 primed $CD4^+$ T cells. Mice were administered twice with increasing dose of recombinant PfMSP-1_{19}, PfMSP-3, crude *P. falciparum* antigen (PfAg), control antigen OVA (25, 50 and 100 µg per mouse) or PBS in CFA/IFA. Cultures were set up 7 days after last immunization. (a) Purified $CD4^+$ T cells from the spleen were stimulated or not stimulated with 100 µg/mL of recall antigen in the presence of syngenic splenic APCS and expression of Ki-67 positive cells in $CD4^+$ T cells were assayed by flow cytometry. Cells were gated on $CD4^+$ T cells and analysed for Ki-67 expression at the times indicated. (b) Purified $CD4^+$ T cells from the spleen were stimulated with titrating dose of recall antigen in the presence of syngenic splenic APCS. The percentage of apoptotic cells among $CD4^+$ T cells were detected, 72 h after stimulation, by staining cells with Annexin V and analysed by flow cytometry. (c) Purified $CD4^+$ T cells from the spleen were stimulated with 100 µg/mL of recall antigen in the presence of syngenic splenic APCS. At indicated time after *in vitro* stimulation with recall Ag, percentage apoptotic cells among $CD4^+$ T cells were detected by staining cells with Annexin V and analysed by flow cytometry. Data are representative of three independent experiments.

low proliferative responses of PfMSP-1_{19} and PfAg-primed $CD4^+$ T cells results from a block in cell cycle progression and increased AICD. In contrast, PfMSP-3 and also OVA primed $CD4^+$ T cells were able to enter the cell cycle after recall stimulation and susceptibility to AICD was delayed till 96 h. After 96 h of antigen stimulation, there was marked increase in the number of apoptotic cells, a time period that correlated with the marked decrease in proliferative response.

We also determined whether apoptosis involved $CD4^+$ or $CD8^+$ T cells or both and B cells in mice primed with PfMSP-1_{19}, PfMSP-3, PfAg and also OVA. Splenocytes from immunized mice were stimulated *in vitro* with recall antigen for

Journal compilation © 2008 Blackwell Publishing Ltd, *Parasite Immunology*, **30**, 497–514

72 h and apoptotic cells among various cell populations were assayed. While majority of the apoptotic cells were T cells (38%), the proportion of B cells that were apoptotic was less compared to T cells (12% vs. 38%, respectively) and that of macrophages and dendritic cells were negligible (< 2·6%). Among T cells, the $CD4^+$ T cells represented the dominant population that was apoptotic compared to $CD8^+$ T cells (data not shown).

We also investigated whether AICD of antigen-primed $CD4^+$ T cells is antigen specific. We found that PfMSP-1_{19} failed to induce apoptosis in PfMSP-3 as well as OVA primed $CD4^+$ T cells and similarly PfMSP-3 failed to induce apoptosis in PfMSP-1_{19} or OVA primed $CD4^+$ T cells and OVA failed to induce apoptosis in PfMSP-1_{19} or PfMSP-3 primed $CD4^+$ T cells (data not shown). However PfAg, which is a crude parasite antigen preparation induced apoptosis in both PfMSP-1_{19} and PfMSP-3 but not in OVA primed $CD4^+$ T cells but only at 1 mg/mL (data not shown). PfAg-induced AICD was significantly lower for $CD4^+$ T cells from PfMSP-3-immunized mice than from PfMSP-1_{19}-immunized mice (data not shown). We next sought to determine the mechanism of apoptosis in PfMSP-1_{19}, PfAg and PfMSP-3 activated $CD4^+$ T cells.

Role of death receptor signalling in PfMSP-1_{19} and PfMSP-3 induced AICD of $CD4^+$ T cells

We next examined the expression of various molecules of the TNF superfamily that may have played a role in the AICD of antigen-primed $CD4^+$ T cells. *Ex vivo* antigen-primed $CD4^+$ T cells expressed increased level of Fas and FasL compared to cells from adjuvant treated mice (Figure 5a,b). $CD4^+$ T cells from PfMSP-3 or OVA primed mice after *in vitro* stimulation with recall antigen showed a time dependent increase in expression of Fas and FasL as determined by changes in the percentage of positive cells (Figure 5c) and fluorescence intensity (Figure 5d) relative to cells from adjuvant control group treated with medium alone. In contrast, no significant changes were observed in the percentage of Fas and FasL positive cells in PfMSP-1_{19} and PfAg primed $CD4^+$ T after *in vitro* stimulation with recall antigen (Figure 5c). While there was slight time dependent increase in the mean fluorescence intensity level of Fas, the fluorescence intensity of FasL remained unchanged in PfMSP-1_{19} and PfAg primed $CD4^+$ T after *in vitro* stimulation with recall antigen (Figure 5d). Expressions of other members of TNF family involved in the apoptosis of T cells, TNFR1, TNFR2, TRAILR1 and TRAILR2 on the surface of Ag-primed $CD4^+$ T cells were not affected by stimulation (data not shown).

To determine whether Fas–FasL, TNF–TNFRs or TRAIL–TRAILRs were involved in AICD, $CD4^+$ T cells from Ag primed mice were treated with competitive inhibitor of Fas–FasL TNF–TNFRs or TRAIL–TRAILRs interaction, the soluble Fas.Fc TNFR.Fc or TRAILR.Fc fusion protein, respectively. Addition of Fas–Fc TNFR.Fc or TRAILR.Fc fusion protein (10 μg/mL) completely blocked anti-Fas, anti-TNFR1 and anti-TRAILR1 mediated apoptosis of naïve $CD4^+$ T cells (data not shown). Treatment with Fas.Fc but not TNFR.Fc or TRAIL.Fc fusion proteins rescued Ag-primed $CD4^+$ T cells from PfMSP-3 and also OVA induced apoptosis (Figure 6). In contrast, addition of the Fas.Fc failed to decrease levels of PfMSP-1_{19} as well as PfAg induced AICD of $CD4^+$ T cells (Figure 6), suggesting that Fas–FasL interaction was not involved in PfMSP-1_{19} or PfAg-mediated apoptosis. Also TNFR and TRAIL did not play any significant role in the induction of apoptosis in malaria antigen primed $CD4^+$ T cells (Figure 6). Together, these results demonstrate that Fas–FasL interaction account for the AICD of PfMSP-3-as well as OVA-primed $CD4^+$ T cell but not essential for the induction of cell death in PfMSP-1_{19} and PfAg-primed $CD4^+$ T cells

Role of the mitochondrial apoptosis pathway in PfMSP-1_{19} and PfMSP-3 induced AICD of $CD4^+$ T cells

It was previously reported that the propensity for activated T cells to die in the absence of Fas or TNFR signalling correlates with a reduction in the Bcl-2 expression relative to Bax (44–46). We next determined whether PfMSP-1_{19} or PfMSP-3 induced AICD of $CD4^+$ T cells correlated with altered expression of anti-apoptotic Bcl-2 and pro-apoptotic Bax proteins Bax. The expression of pro-apoptotic protein Bax increased with time in both PfMSP-1_{19} and PfAg primed $CD4^+$ T cells after *in vitro* stimulation with recall antigen (Figure 7a), indicating that increase in Bax level was probably associated with apoptosis of these antigen primed $CD4^+$ T cells. The increase in the percentage and MFI of Bax-containing cells was more prominent in PfAg-primed $CD4^+$ T cells compared to PfMSP-1_{19}-primed $CD4^+$ T cells (Figure 7a). While stimulation of antigen primed $CD4^+$ T cells with recall PfMSP-1_{19} and PfAg drastically increased the expression of pro-apoptotic Bax, there was no significant change in the expression of anti-apoptotic Bcl-2 molecule (Figure 7b). The level of both Bcl-2 and Bax was unaffected by *in vitro* stimulation of PfMSP-3 as well as OVA primed $CD4^+$ T cells with recall antigen (Figure 7a,b). The expressions of other Bcl-2 molecules in Ag-primed $CD4^+$ T cells remained unchanged after *in vitro* stimulation with recall antigen (data not shown). Given that the ratio of Bax : Bcl-2 determines the susceptibility to cell death rather than the level of individual protein (45), we calculated the Bax : Bcl-2 ratio using the mean fluorescence intensity of Bax and Bcl-2. Upon stimulation with PfMSP-1_{19} and PfAg but not with PfMSP-3 there was time dependent increase in Bax : Bcl-2 protein ratios in primed $CD4^+$ T cells (Figure 7c). Further subcellular fractionation study revealed that pro-apoptotic Bax was found to be associated with the mitochondrial and

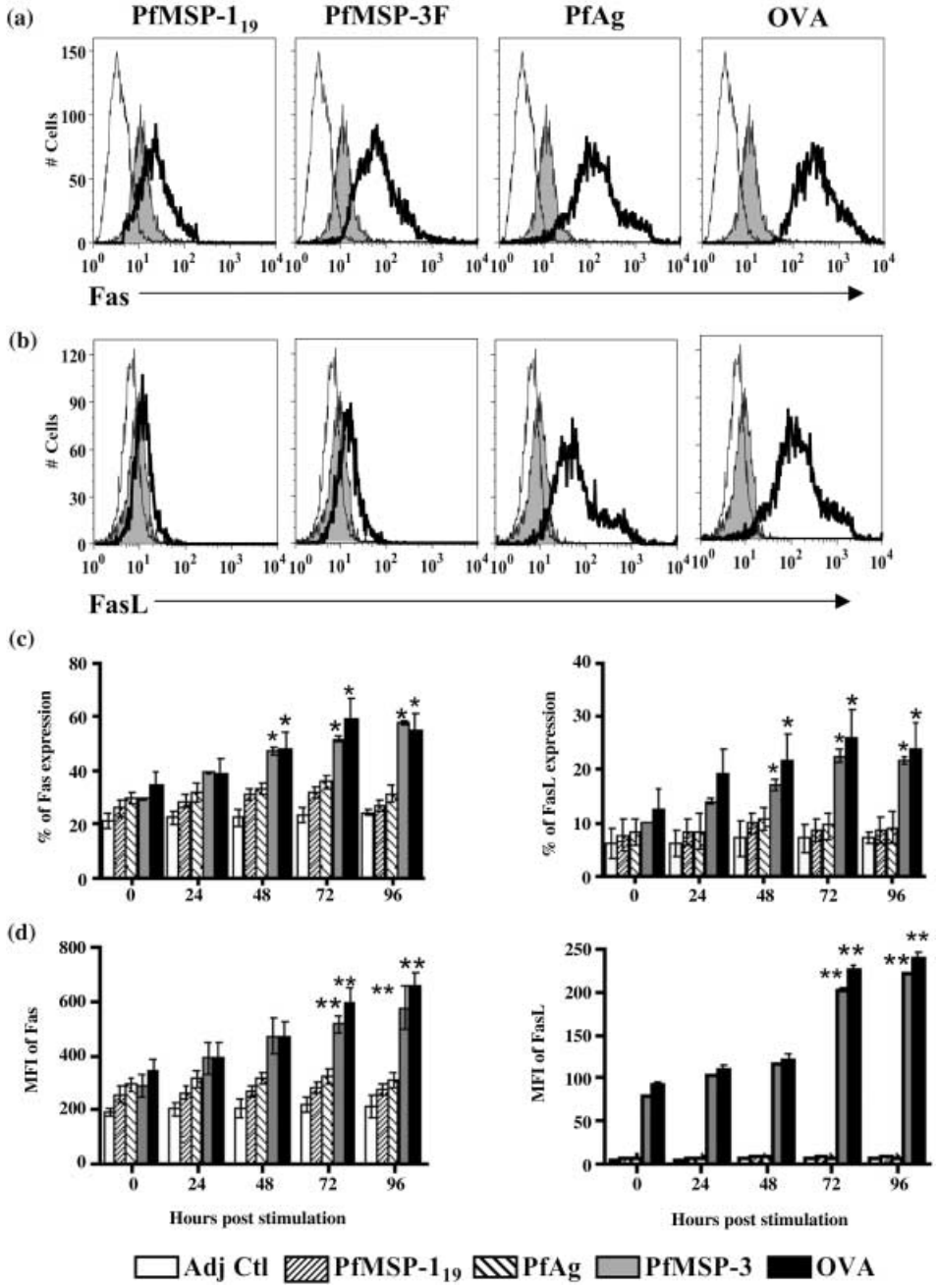

Figure 5 Expression of CD95 and CD95L on PfMSP-1_{19} and PfMSP-3 primed $CD4^+$ T cells. Mice were administered twice with increasing dose of recombinant PfMSP-1_{19}, PfMSP-3, crude *P. falciparum* antigen (PfAg), control antigen OVA (25, 50 and 100 mg per mouse) or PBS in CFA/IFA. (a) At day 7 after last immunization, splenic cells from Ag primed mice as well as from control adjuvant control mice (shaded curves) were stained with anti-CD4 vs. anti-CD95 or anti-CD95L. $CD4^+$ T cells were gated, and their levels of CD95 or CD95L are shown as single-colour histograms. Thick line represents $CD4^+$ T cells from primed mice, grey filled histogram represents $CD4^+$ T cells from adjuvant control mice, and thin grey line represents corresponding isotype-matched control. Data are representative of two to four independent experiments. (b, c) $CD4^+$ T cells from Ag primed mice were purified 7 days after last immunization and stimulated or not stimulated *in vitro* with 100 μg/mL of recall antigen plus splenic APC. At indicated time after stimulation, expression of CD95 and CD95L were determined by flow cytometry on $CD4^+$ gated cells. (b) Percentages of CD95 and CD95L among splenic $CD4^+$ T cells and (d) and the mean fluorescence intensity (MFI) of staining of CD95 and CD95L are shown. MFI value has been corrected for the mean fluorescence intensity obtained with an isotype-matched control mAb. Data from five experiments were pooled to obtain the mean ± SD. *, $P < 0{\cdot}01$, **, $P < 0{\cdot}001$ are the statistically significant difference for each group compared to adjuvant control group indicated above the bars.

Journal compilation © 2008 Blackwell Publishing Ltd, *Parasite Immunology*, **30**, 497–514

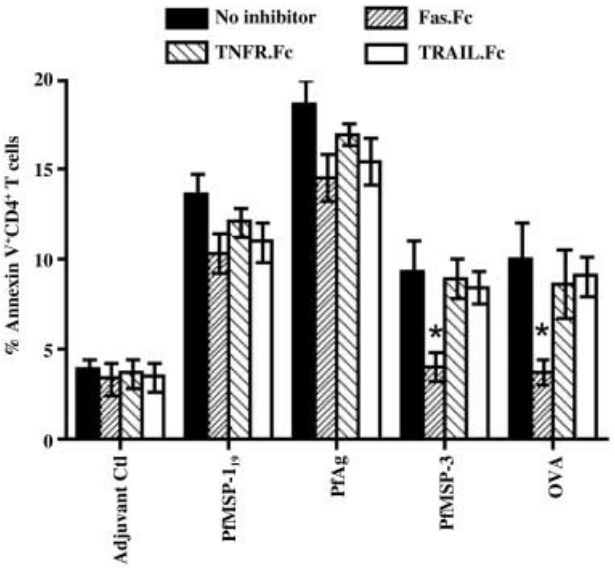

Figure 6 Role of death receptor signalling in AICD of PfMSP-1_{19} and PfMSP-3 primed $CD4^+$ T cells. $CD4^+$ T cells isolated from PfMSP-1_{19}, PfAg, PfMSP-3, OVA and adjuvant treated mice were stimulated or not stimulated *in vitro* with recall antigen plus splenic APCs. Fas–Fc TNFR.Fc or TRAILR.Fc fusion proteins (1 μg/mL) were added at the beginning of the culture and maintained throughout the culture. After 72 h, percentage of apoptotic cells among $CD4^+$ T cells were detected by staining cells with Annexin V FITC and analysed by flow cytometry. Data from five experiments were pooled to obtain the mean ± SD. *, $P < 0{\cdot}02$ is the statistically significant difference indicated above the bars.

not with the cytosolic subcellular fractions of PfMSP-1_{19} and PfAg primed $CD4^+$ T cells (Figure 8). One major consequence of Bax translocation to mitochondria is the release of cytochrome c. We next assayed for the release of cytochrome c from the mitochondria of PfMSP-1_{19} and PfAg primed $CD4^+$ T cells. We found that stimulation of PfMSP-1_{19} and PfAg-primed $CD4^+$ T cells with recall antigen induced cytochrome c release from mitochondria into cytosol, but no cytosolic cytochrome *c* could be detected in the PfMSP-3 or OVA-primed $CD4^+$ T cells upon treatment with recall antigen plus APCs. These results demonstrate that pro-apoptotic members of the Bcl-2 protein family through mitochondrial dependent pathway modulated PfMSP-1_{19} and PfAg induced AICD of $CD4^+$ T cells.

AICD of $CD4^+$ T cells induced by recombinant *Plasmodium falciparum* antigens are caspases dependent

Caspases, the central elements of the Fas- and mitochondria-mediated apoptotic pathways, initiate a cascade of events that end in death of the cells (47). To determine whether caspases were involved, we compared the effect of different caspase inhibitors on AICD of $CD4^+$ T cells induced by different malarial antigens. As shown in Figure 9a, z-VAD-fmk, a general caspase inhibitor effectively blocked AICD in antigen primed $CD4^+$ T cells restimulated with recall PfMSP-1_{19}, PfAg, PfMSP-3 or OVA. Stimulation of Ag-primed $CD4^+$ T cells in the presence of specific inhibitors of caspase-3 (z-DEVD-fmk) and caspase-8 (z-IETD-fmk) blocked PfMSP-3 and also OVA-induced AICD. On the other hand, specific caspase-9 inhibitor (z-LEHD-fmk) caspase-3 inhibitor (z-DEVD-fmk) and caspase-8 inhibitor (z-IETD-fmk) had a strong protective effect against both PfMSP-1_{19}- and PfAg-induced AICD of $CD4^+$ T cells (Figure 9a).

In next set of experiments, we determined the hierarchy of the caspase cascade in PfMSP-1_{19} and PfMSP-3-induced AICD of $CD4^+$ T cells. By using an enzymatic colourimetric assay, we evaluated caspase activity in $CD4^+$ T cell lysates by using specific fluorescence substrates (Ac-IETD-pNA, Ac-LEHD-pNA and Ac-DEVD-pNA) in the absence or presence of caspase inhibitors (Figure 9b). Compared with $CD4^+$ T cells from adjuvant control mice, $CD4^+$ T cells from PfMSP-1_{19}-, PfMSP-3- PfAg- and OVA-primed mice expressed increased caspase activation after *in vitro* stimulation with recall antigen (Figure 9b). $CD4^+$ T cells from PfMSP-1_{19}- and PfAg-primed mice expressed increased caspase-9, caspase-3 and caspase-8 activities in response to recall stimulation (Figure 9b). Presence of z-LEHD-fmk during stimulation prevented activation of all three caspases (caspase-9, caspase-3 and caspase-8), z-DEVD-fmk prevented activation of both caspase-3 and caspase-8, whereas the z-IETD-fmk blocked the activation of caspase-8 only (Figure 9b). Both z-DEVD-fmk and z-IETD-fmk failed to block the activation of caspase-9 (Figure 9b). In contrast, $CD4^+$ T cells from PfMSP-3 and OVA-primed mice expressed increased caspase-8 and caspase-3 activities upon *in vitro* stimulation with recall antigen (Figure 9b). In these cells, presence of z-IETD-fmk during recall stimulation blocked the activation of both caspase-8 and caspase-3 whereas z-DEVD-fmk blocked the activation of caspase-3 only (Figure 9b) whereas z-LEHD-fmk had almost no effect, indicating that caspase-9 activation was dispensable for AICD of PfMSP-3 and OVA-primed $CD4^+$ T cells.

Since PfMSP-3, PfMSP-1_{19} and PfAg primed $CD4^+$ T cells were found to express different levels of Fas and FasL on the cell surface after stimulation (Figure 5), we determined whether interference in Fas-FasL interaction affected caspase activation in these antigen-primed $CD4^+$ T cells. Caspase enzymatic activity was again determined in the cell lysates by colourimetric assay (Figure 10). As we had shown in Figure 6, Fas-Fc inhibited PfMSP-3 as well as OVA-induced AICD, addition of soluble Fas–Fc fusion protein to the culture prevented PfMSP-3-mediated activation of caspase-8 and caspase-3 (Figure 10). In contrast, Fas-Fc had

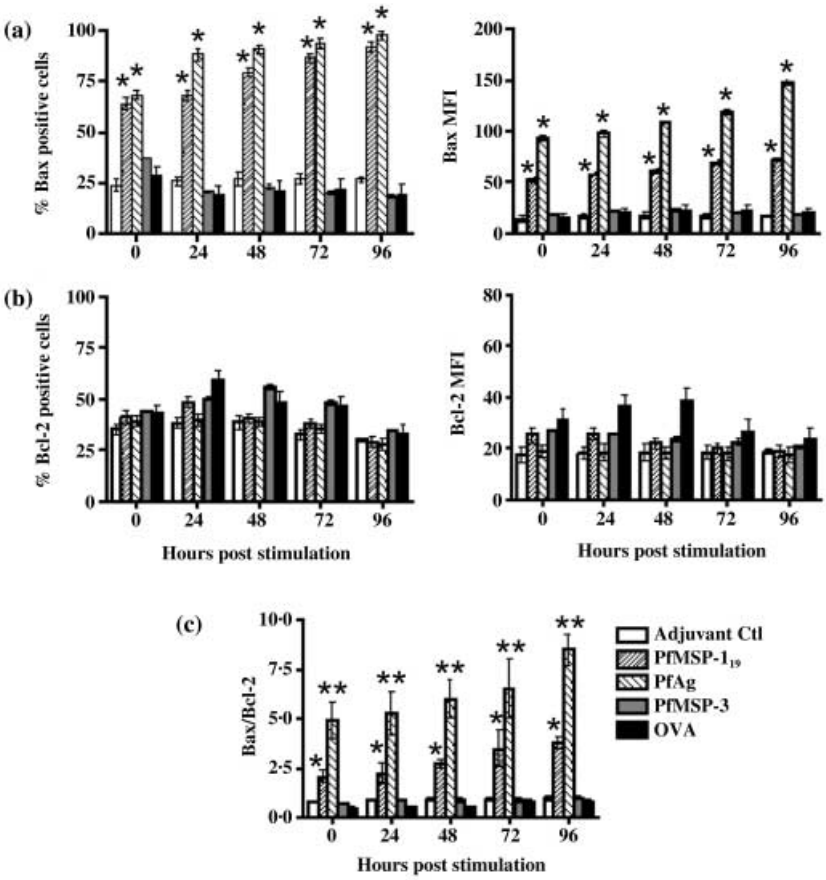

Figure 7 Expression of Bcl-2 and Bax on PfMSP-1_{19} and PfMSP-3 primed CD4+ T cells. CD4+ T cells from Ag primed mice were purified 7 days after last immunization and stimulated or not stimulated *in vitro* with 100 μg/mL of recall antigen plus splenic APC. At indicated time after stimulation, intracellular expression of Bax and Bcl-2 were determined by flow cytometry on CD4+ CD44+ gated cells. (b) Percentages of Bax and Bcl-2 among splenic CD4+ T cells and (c) and the mean fluorescence intensity (MFI) of staining of Bax and Bcl-2 are shown. MFI value has been corrected for the mean fluorescence intensity obtained with an isotype-matched control mAb. Data from five experiments were pooled to obtain the mean ± SD. *, $P < 0{\cdot}01$ is the statistically significant difference for each group compared to adjuvant control group indicated above the bars. C, At indicated time after *in vitro* stimulation with recall Ag, ratio of Bax : Bcl-2 protein expression (fluorescence intensity) among various antigens primed CD4+ T cells was calculated. Data from three experiments were pooled to obtain the mean ± SD. *, $P < 0{\cdot}01$, **, $P < 0{\cdot}001$ are the statistically significant difference for each group compared to adjuvant control group indicated above the bars.

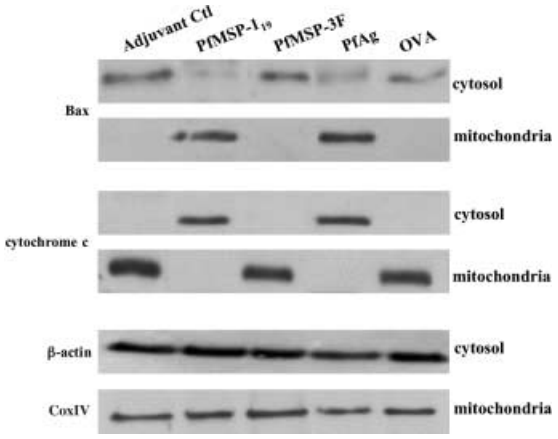

Figure 8 Movement of Bax or cytochrome c to or from mitochondria in PfMSP-1_{19} and PfMSP-3 primed CD4+ T cells. CD4+ T cells from Ag primed mice were purified 7 days after last immunization and stimulated or not stimulated *in vitro* with 100 μg/mL of recall antigen plus splenic APC. CD4+ T cells were harvested, 72 h after stimulation, and cytosolic and mitochondrial Bax and cytochrome *c* levels were determined by Western blot analysis. Markers for the respective fractions of mitochondria (CoxIV) and cytosol (β-actin) are also shown. Results are representative of two independent experiments.

little effect on the AICD of CD4+ T cells induced by PfMSP-1_{19} or PfAg (Figure 6). Consistent with these results, addition of Fas.Fc fusion protein in the culture medium had little effect on the activation of caspase-9, caspase-8 and caspase-3 in CD4+ T cells stimulated PfMSP-1_{19} or PfAg (Figure 10). These results indicate that PfMSP-1_{19} and also PfAg induced AICD of CD4+ T cells was via the mitochondrial death pathway while PfMSP-3 and OVA induced AICD of CD4+ T cells depended on the Fas–FasL interactions. Our data demonstrate that different *P. falciparum* merozoite surface antigens can trigger diverse programs of AICD in CD4+ T cells.

DISCUSSION

In this study we sought to determine the fate of CD4+ T cells (proliferation and activation induced cell death) in mice immunized with the blood stage recombinant merozoite surface antigens, PfMSP-1_{19} and PfMSP-3 and the molecular events underlying the process of AICD of antigen primed CD4+ T cells. It has been established that in response to infection or immunization, Ag-reactive responses are normally related with the proliferation of Ag-specific T cells that differentiate

Journal compilation © 2008 Blackwell Publishing Ltd, *Parasite Immunology*, **30**, 497–514

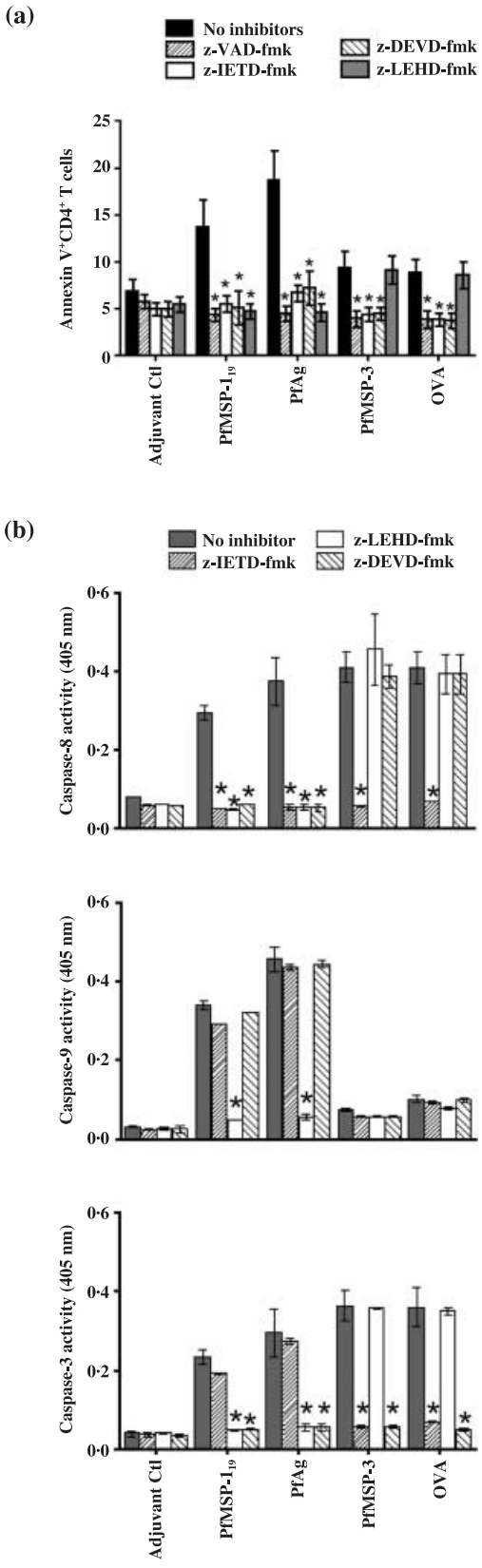

to an effector phenotype (2). This oligoclonal expansion of T cells is counterbalanced by apoptotic cell death of the activated CD4 T cells upon restimulation (1,3). This form of apoptosis, called AICD is an active cell suicide mechanism of widespread biological importance that constitutes the physiological response of normal T cells to activation and is believed to control the number of Ag-stimulated T cells during the immune response. Our *in vitro* results extend these findings by demonstrating that during immunization with nonreplicating immunogens like OVA or recombinant *P. falciparum* blood stage antigens, activated CD4$^+$ T cells when restimulated with Ag through TCR undergo AICD.

CD4$^+$ T cells from mice primed with increasing dose of PfMSP-1$_{19}$, PfMSP-3, crude parasite antigen (PfAg) as well as OVA-primed show activated phenotype and expressed high levels of the acute activation markers CD69, CD25 as well as CD44 and decrease CD62L and CD45RB expression on the cell surface. Despite activated phenotype, antigen-primed CD4$^+$ T cells exhibit different capacities to proliferate in response to recall stimulation. We found that the differences in the proliferative response of antigen-primed CD4$^+$ T cells to recall antigens was not due to TCR down-regulation as CD4$^+$ T cells from all the groups expressed similar level of surface TCR (data not shown). All *ex vivo* antigen-primed CD4$^+$ T cells expressed different level of Ki-67, a marker indicative of ongoing proliferation, which perhaps could account for high background proliferative response. Data presented here provide evidence that *ex vivo* PfMSP-1$_{19}$ and PfAg-primed CD4$^+$ T cells expressed low levels of Ki-67 reflecting an ongoing response that was initiated *in vivo* but fail to undergo cell cycle progression after *in vitro* Ag re-stimulation. The low proliferation of PfMSP-1$_{19}$ and PfAg primed CD4$^+$ T cells is possibly due to cell cycle arrest of CD4$^+$ T cells. The failure of PfMSP-1$_{19}$ and PfAg-primed CD4$^+$ T cells

Figure 9 AICD of PfMSP-1$_{19}$ and PfMSP3 primed CD4$^+$ T cells is caspase dependent. A and B, CD4$^+$ T cells from Ag primed mice were purified 7 days after last immunization and stimulated or not stimulated *in vitro* with 100 μg/mL of recall antigen plus splenic APC. pan-specific caspase inhibitor Z-VAD-fmk (50 μm), caspase 3 inhibitor (z-DEVD-fmk, 50 μm), caspase 8 inhibitor (Z-IETD-fmk, 50 μm), caspase 9 inhibitor (Z-LEHD-fmk, 50 μm), or no inhibitor were added at the beginning of the culture. (a) 72 h after stimulation, percentage of apoptotic cells among CD4$^+$ T cells were detected by staining cells with Annexin V FITC and analysed by flow cytometry. Data from three experiments were pooled to obtain the mean ± SD. *, $P < 0{\cdot}05$ significant difference between no inhibitor- and presence of inhibitor for each group indicated above the bars. (b) 72 h after stimulation, CD4$^+$ T cells were assessed for caspase-8, caspase-9 and caspase-3-like activity by colourimetric enzyme assay using specific substrate (Ac-IETD-pNA, -Ac-LEHD-pNA and Ac-DEVD-pNA) as described in Materials and Methods. Results are depicted as mean ± SE of three independent experiments. *, $P < 0{\cdot}05$ significant difference between no inhibitor- and presence of inhibitor for each group indicated above the bars.

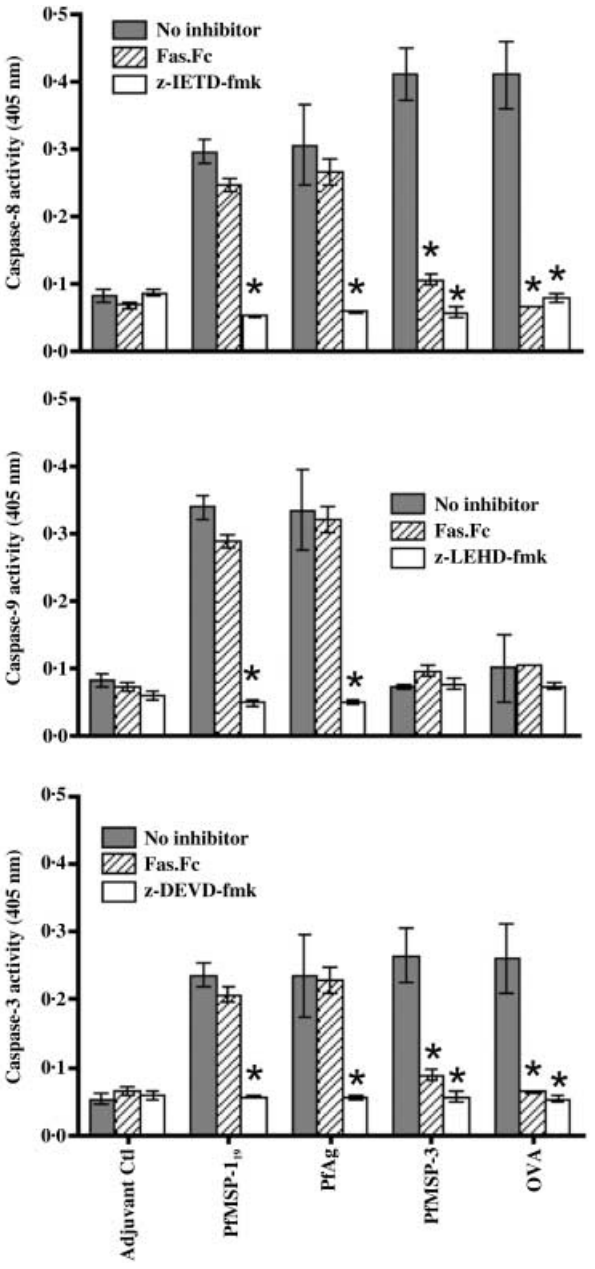

Figure 10 Role of Fas.Fc in caspase-8, casapse-9 and caspase-3 activities in PfMSP-1_{19} and PfMSP-3 primed CD4+ T cells. CD4+ T cells from Ag primed mice were purified 7 days after last immunization and stimulated or not stimulated *in vitro* with 100 μg/mL of recall antigen plus splenic APC. Fas-Fc fusion proteins (1 μg/mL) and caspase inhibitor (50 μM) or inhibitors were added at the beginning of the culture and maintained throughout the culture. 72 h after stimulation, CD4+ T cells were assessed for caspase-8, caspase-9 and caspase-3-like activity by colourimetric enzyme assay using specific substrate (Ac-IETD-pNA, -Ac-LEHD-pNA and Ac-DEVD-pNA) as described in Materials and Methods. Results are depicted as mean ± SE of three independent experiments. *, $P < 0{\cdot}001$ significant difference between no inhibitor- and presence of inhibitor for each group indicated above the bars.

to progress through cell cycle while still expressing activation phenotype could be related to the increased activation induced cell death. The kinetics of cell cycle arrest and AICD in PfMSP-1_{19} and PfAg-primed CD4+ T cells show that the block in cell cycle progression is detected between 48 and 72 h and maximal AICD between 72 and 96 h. Based on these observations, we may conclude that cell cycle arrest perhaps is the principal cause of PfMSP-1_{19} and PfAg-primed CD4+ T cells to become susceptible to AICD. The low *in vitro* recall responses of PfMSP-1_{19} and PfAg primed CD4 T cells are consistent with published data (48). Quin *et al.* (48) had shown that MSP-1_{19} of the mouse malaria parasite *Plasmodium chabaudi chabaudi* (AS) also stimulate a weak CD4 T cell response when compared to the response to a more structurally simple region of the molecule and they had attributed the low response to processing within distinct MHC class II pathways.

In contrast, PfMSP-3 primed CD4+ T cells and also OVA-primed CD4+ T cells did not show any impairment in the ability to enter the cell cycle and expressed increased level of Ki-67. PfMSP-3-activated CD4+ T cells underwent a burst of proliferation that was followed by apoptosis. Together, these findings indicate that PfMSP-3 does exert stimulatory effects on CD4+ T cells and inhibits TCR-induced cell cycle progression rather late after T cell activation. Indeed, the increase in survival of PfMSP-3-primed CD4+ T cells is probably due to the maintenance of the proliferative capacity of these activated T cells. Activated T cells are programmed to acquire susceptibility to apoptosis only after a given number of cell divisions (49). Also mature T cells in the G1 phase of the cell cycle are refractory to receptor-induced apoptosis, whereas T cells that have progressed to the S phase are susceptible (50). Stimulation of proliferating T cells has been shown to result in AICD (51). It is tempting to speculate that AICD of PfMSP-3-primed CD4+ T cells is regulated in this way so as to allow T cells to expand and perform their effector functions, while at the same time ensuring homeostasis.

A major observation from this study is that splenic CD4+ T cells from primed mice show the phenotype and optimal cell cycle progression of activated effector rather than resting memory CD4+ T cells. Since no proliferation is observed in the absence of APC or by naïve CD4+ T cells suggests that PfMSP-1_{19} and PfMSP-3 and also crude parasite extract did not have any mitogenic effect on CD4+ T cells.

The main objective of the study was to determine which cell death pathways were operative in PfMSP-1_{19} and PfMSP-3-induced AICD of CD4+ T cells. Results presented in this study demonstrate that PfSMP-1_{19} and PfMSP-3 as well crude *P. falciparum* antigen resulted in sequential T cell activation, proliferation followed by cell death via AICD in a dose- and time-dependent manner. AICD is one of the mechanisms for eliminating clonally expanded antigen-specific T cells (52,53). In this study we demonstrate that malaria Ag-reactive CD4+

Journal compilation © 2008 Blackwell Publishing Ltd, *Parasite Immunology*, **30**, 497–514

T cells are susceptible to antigen-mediated AICD which is consistent with the observations of previous studies indicating that $CD4^+$ T cells from infected individuals readily undergo apoptosis upon *in vitro* stimulation with parasite lysate (16,17). Our results show that blood stage antigens, PfMSP-1_{19} and PfMSP-3 trigger different AICD pathways in antigen primed $CD4^+$ T cells. PfMSP-3 sensitizes $CD4^+$ T cells toward CD95-mediated, caspase-8-dependent cell death. PfMSP-3 primed $CD4^+$ T cells show significant up-regulation and persistent expression of Fas and FasL and blocking Fas–FasL interactions abrogated PfMSP-3-mediated AICD of $CD4^+$ T cells. Furthermore, our study provide evidence that the PfMSP-3-induced AICD of $CD4^+$ T cells is mediated by activation of caspase-8 and caspase-3 that are central to death receptor apoptosis signalling pathways (54). Interrupting Fas–FasL interaction significantly blocked activation of caspase-8 and caspase-3 and reduced the AICD of PfMSP-3-primed $CD4^+$ T cells. These results suggest that death receptor signalling play a predominant role in PfMSP-3 induced AICD of $CD4^+$ T cells. Furthermore, and consistent with previous reports, our studies indicate that the OVA also induced Fas-mediated AICD in Ag-activated $CD4^+$ T cells (55).

PfMSP-1_{19}- as well as PfAg-primed $CD4^+$ T cells are relatively insensitive to Fas-mediated cell death since blocking this pathway did not increase cell survival or prevent caspase activation. Instead, our studies indicate that the AICD in these activated cells may involve engagement of mitochondria apoptosis signalling pathway. Both pro- and anti-apoptotic members of the Bcl-2 protein family largely regulate the mitochondrial death pathway (56). In many instances it has been reported that Bax expression is up-regulated during apoptosis in several types of cells, together with the decrease of the Bcl-2 protein level (57). But it is the ratio rather than expression level of individual anti- and pro-apoptotic protein that appears to be an important determinant for apoptosis: lower ratio favours cell survival, whereas higher Bax : Bcl-2 ratio promotes cell death in several cell types including $CD4^+$ T cells (58). The expression profile of Bcl-2 and Bax expression in PfMSP-1_{19}- and PfAg-primed $CD4^+$ T cells suggests that up-regulation of Bax protein and resulting change of Bax : Bcl-2 protein ratio may be an important determinant for the induction of AICD. The translocation of the pro-apoptotic molecule Bax to mitochondria possibly mediated the release of cytochrome c and regulated the intrinsic apoptosis pathway involving the mitochondria (59). Consistent with this observation, Bax was found to be predominantly associated with the mitochondrial fraction and cytochrome *c* was predominantly detected in the cytosolic fraction of the both PfMSP-1_{19}- and PfAg-activated $CD4^+$ T cells. Blocking caspase-9 activation with a specific inhibitor, z-LEHD-fmk, reduced both PfMSP-1_{19} and PfAg induced AICD of Ag-primed $CD4^+$ T cells, further demonstrated that the mitochondrial cascade played a significant role in PfMSP-1_{19}- and PfAg-induced apoptosis of the $CD4^+$ T cells. Xu *et al.* (42) had demonstrated that the depletion of parasite-specific $CD4^+$ T cells was independent of TNF or Fas molecules but the molecular mechanism was not established. Recently, Guha *et al.* (60) had shown that mechanistic basis of hepatic dysfunction during blood stage infection involves simultaneous Bcl-2 down-regulation and Bax up-regulation and reduced the Bcl-2 : Bax ratio, resulting in the activation and translocation of Bax to mitochondria. Bax translocation to mitochondria through opening of permeability transition pores induced release of apoptotic inducing proteins, such as cytochrome c into cytosol. Cytochrome c activates caspase-3, which finally executed the apoptosis of hepatocytes. Thus, PfMSP-1_{19} and PfSMP-3 primed $CD4^+$ T cells appear to use distinct mechanisms of AICD to limit excessive clonal expansion following a productive response, while permitting important effector functions to be expressed.

In this study, we demonstrate that different merozoite surface antigens are capable of modulating not only the course of $CD4^+$ T cell activation but also trigger diverse apoptotic programs of AICD; however, it is not clear what factors determine these programs. Recently, it has been shown that T cells from *P. falciparum* infected individuals are conditioned *in vivo* to die by apoptosis *in vitro* (28–31). It is thus likely that a major and universal mechanism of parasite-induced immune suppression may be the stimulation of $CD4^+$ T cells into apoptotic death upon antigenic challenge. Although apoptosis during malaria infection may help in attenuating acute antiparasite responses, at the same time it may also lead to defective immune responses and lead to unrestricted parasitemia and damage of host tissues (41,42). The blood stage parasite antigens that interact with the host cells' apoptosis signalling cascades may have impact on the course of disease. Thus, the current study could provide a model for investigating the molecular mechanisms underlying the deletion of whole parasite-specific proliferative $CD4^+$ T cells and develop strategies to enhance immunity following immunization. The practical implication of predicting the effects of various potential malaria vaccine candidates on the $CD4^+$ T cell activation, proliferation and apoptosis will add to our understanding the efficacy of antigen(s) based malaria vaccine development. These issues are of utmost importance in malaria immunity and antigen(s) based malaria vaccine development.

ACKNOWLEDGEMENTS

This work was supported by grants from Indian Council of Medical Research (63/176/2002-BMS. IRIS No. 2001-041-40) to P.M. and by the institutional core grant from ICGEB, New Delhi.

REFERENCES

1 Green DR, Droin N & Pinkoski M. Activation-induced cell death in T cells. *Immunol Rev* 2003; **193**: 70–81.
2 Van Parijs L & Abbas AK. Homeostasis and self-tolerance in the immune system: turning lymphocytes off. *Science* 1998; **280**: 243–248.
3 Radvanyi LG, Mills GB & Miller RG. Religation of the T cell receptor after primary activation of mature T cells inhibits proliferation and induces apoptotic cell death. *J Immunol* 1993; **150**: 5704–5715.
4 van Parijs L, Ibraghimov A & Abbas AK. The roles of costimulation and Fas in T-cell apoptosis and peripheral tolerance. *Immunity* 1996; **4**: 321–328.
5 Lenardo MJ. The molecular regulation of lymphocyte apoptosis. *Semin Immunol* 1997; **9**: 1–5.
6 Hildeman DA, Zhu YN, Mitchell TC, Kappler J & Marrack P. Molecular mechanisms of activated T cell death *in vivo*. *Curr Opin Immunol* 2002; **14**: 354–359.
7 Krammer PH. CD95s deadly mission in the immune system. *Nature* 2002; **407**: 789–795.
8 Krueger A, Fas SC, Baumann S & Krammer PH. The role of CD95 in the regulation of peripheral T-cell apoptosis. *Immunol Rev* 2003; **193**: 58–69.
9 Lavrik I, Golks A & Krammer PH. Death receptor signaling. *J Cell Sci* 2005; **118**: 265–267.
10 Ashkenazi A & Dixit VM. Apoptosis control by death and decoy receptors. *Curr Opin Cell Biol* 1999; **11**: 255–260.
11 Green DR & Reed JC. Mitochondria and Apoptosis. *Science* 1998; **281**: 309–1312.
12 Susin SA, Zamzami N & Kroemer G. Mitochondria as regulators of apoptosis: doubt no more. *Biochim Biophys Acta* 1998; **1366**: 151–165.
13 Willis S, Day CL, Hinds MG & Huang DC. The Bcl-2-regulated apoptotic pathway. *J Cell Sci* 2003; **116**: 4053–4056.
14 Gross A, McDonnell JM & Korsmeyer SJ. Bcl-2 family members and the mitochondria in apoptosis. *Genes Dev* 1999; **13**: 1899–1911.
15 Good MF. Vaccine-induced immunity to malaria parasites and the need for novel strategies. *Trends Parasitol* 2005; **21**: 29–34.
16 Good MF, Stanisic D, Xu H, Elliott S & Wykes M. The immunological challenge to developing a vaccine to the blood stages of malaria parasites. *Immunol Rev* 2004; **201**: 254–267.
17 Langhorne J, Quin SJ & Sanni LA. Mouse models of blood-stage malaria infections: immune responses and cytokines involved in protection and pathology. *Chem Immunol* 2002; **80**: 204–228.
18 Achtman AH, Bull PC, Stephens R & Langhorne J. Longevity of the immune response and memory to blood-stage malaria infection. *Curr Top Microbiol Immunol* 2005; **297**: 71–102.
19 Ndungu FM, Urban BC, Marsh K & Langhorne J. Regulation of immune response by *Plasmodium*-infected red blood cells. *Parasite Immunol* 2005; **27**: 373–384.
20 Hisaeda H, Yasutomo K & Himen K. Malaria: immune evasion by parasites. *Int J Biochem Cell Biol* 2005; **37**: 700–706.
21 Langhorne J, Cross C, Seixas E, Li C & Weid TVD. A role for B cells in the development of T helper function in a malaria infection in mice. *Proc Natl Acad Sci USA* 1998; **95**: 1730–1734.
22 van der Heyde HC, Elloso MM, Chang WL, Pepper BJ, Batchelder J & Weidanz WP. Expansion of the gammadelta T cell subset *in vivo* during bloodstage malaria in B cell-deficient mice. *J Leukoc Biol* 1996; **60**: 221–229.
23 von der Weid T & Langhorne J. Altered response of CD4 T cell subsets to *Plasmodium chabaudi chabaudi* in B cell-deficient mice. *Int Immunol* 1993; **5**: 1343–1348.
24 Ho M, Webster HK, Green B, Looareesuwan S, Kongchareon S & White NJ. Defective production of and response to IL-2 in acute human *falciparum* malaria. *J Immunol* 1988; **141**: 2755–2759.
25 Riley EM, Jobe O, Blackman M, Whittle HC & Greenwood BM. *Plasmodium falciparum* schizont sonicates suppress the lymphoproliferative response to mitogens and antigens in malaria-immune adults. *Infect Immun* 1989; **57**: 3181–3188.
26 Ramharter M, Willheim M, Winkler H, *et al*. Cytokine profile of *Plasmodium falciparum*-specific T cells in non-immune malaria patients. *Parasite Immunol* 2003; **25**: 211–219.
27 Farouk SE, Shen J, Tangteerawatana P, Bolad A, Berzins K & Troye-Blomberg M. Analysis of T-cell responses in malaria-exposed and non-exposed donors using *Plasmodium falciparum* asexual blood stages enriched by a simple centrifugation method. *Acta Trop* 2006; **97**: 42–49.
28 Toure-Balde A, Sarthou JL, Aribot A, *et al*. *Plasmodium falciparum* induces apoptosis in human mononuclear cells. *Infect Immun* 1996; **64**: 744–750.
29 Balde AT, Aribot A, Tall A, Spiegel A & Roussilhon C. Apoptosis modulation in mononuclear cells recovered from individuals exposed to *Plasmodium falciparum* malaria. *Parasite Immunol* 2000; **22**: 307–318.
30 Kemp K, Akanmori BD, Adabayeri V, *et al*. Cytokine production and apoptosis among T cells from patients under treatment for *Plasmodium falciparum* malaria. *Clin Exp Immunol* 2002; **12**: 151–157.
31 Riccio EK, Junior IN, Riccio LR, *et al*. Malaria associated apoptosis is not significantly correlated with either parasitemia or the number of previous malaria attacks. *Parasitol Res* 2003; **90**: 9–18.
32 Helmby H, Jonsson G & Troye-Blomberg M. Cellular changes and apoptosis in the spleens and peripheral blood of mice infected with blood-stage *Plasmodium chabaudi chabaudi* AS. *Infect Immun* 2000; **68**: 1485–1490.
33 Hirunpetcharat C & Good MF. Deletion of *Plasmodium berghei*-specific CD4+ T cells adoptively transferred into recipient mice after challenge with homologous parasite. *Proc Natl Acad Sci USA* 1998; **95**: 1715–1720.
34 Holder AA. Proteins on the surface of the malaria parasite and cell invasion. *Parastiology* 1994; **105**: S5–S18.
35 Good MF & Doolan DL. Immune effector mechanisms in malaria. *Curr Opin Immunol* 1999; **11**: 412–415.
36 Holder AA, Guevara Patino JA, Uthaipibull C, *et al*. Merozoite surface protein 1, immune evasion, and vaccines against asexual blood stage malaria. *Parassitologia* 1999; **41**: 409–414.
37 Ling IT, Ogun SA & Holder AA. Immunization against malaria with a recombinant protein. *Parasite Immunol* 1994; **16**: 63–67.
38 McColl DJ, Silva A, Foley M, *et al*. Molecular variation in a novel polymorphic antigen associated with *Plasmodium falciparum* merozoites. *Mol Biochem Parasitol* 1994; **68**: 53–67.
39 Oeuvray C, Bouharoun-Tayoun H, Gras-Masse H, *et al*. Merozoite surface protein3: a malaria protein inducing antibodies that promote *Plasmodium falciparum* killing by cooperation with blood monocytes. *Blood* 1994; **84**: 1594–1602.
40 Bouharoun-Tayoun H, Attanah P, Sabchareon A, Chongsuphajaisiddhi T & Druilhe P. Antibodies that protect humans against *Plasmodium falciparum* blood stages do not on their own inhibit parasite growth and invasion *in vitro*, but act in cooperation with monocytes. *J Exp Med* 1990; **172**: 1633–1641.

41 Wipasa J, Xu H & Good MF. Apoptotic deletion of Th cells specific for the 19-kDa carboxyl-terminal fragment of merozoite surface protein 1 during malaria infection. *J Immunol* 2001; **167**: 3903–3909.
42 Xu H, Wipas J, Yan H, *et al*. The mechanism and significance of deletion of parasite-specific CD4 T cells in malaria infection. *J Exp Med* 2002; **195**: 881–892.
43 Gerdes J, Lemke H, Baisch H, Wacker HH, Schwab U & Stein H. Cell cycle analysis of a cell proliferation-associated human nuclear antigen defined by the monoclonal antibody Ki-67. *J Immunol* 1984; **133**: 1710–1715.
44 Korsmeyer SJ. Bcl-2 gene family and the regulation of programmed cell death. *Cancer Res* 1999; **59**(Suppl.): S1693–S1700.
45 Oltvai ZN, Millman CL & Korsmeyer SJ. Bcl-2 heterodimerixes *in vivo* with a conserved homolog, Bax, that accelerates programmed cell death. *Cell* 1993; **74**: 609–619.
46 Kroemer G. The proto-oncogene Bcl-2 and its role in regulating apoptosis. *Nat Med* 1997; **3**: 614–620.
47 Nicholson DW. Caspase structure, proteolytic substrates, and functions during apoptotic cell death. *Cell Death Differ* 1999; **6**: 1028–1042.
48 Quin SJ, Seixas EM, Cross CA, *et al*. Low CD4(+) T cell responses to the C-terminal region of the malaria merozoite surface protein-1 may be attributed to processing within distinct MHC class II pathways. *Eur J Immunol* 2001; **31**: 72–81.
49 Renno T, Attinger A, Locatelli S, Bakker T, Vacheron S & MacDonald HR. Apoptosis of superantigen-activated t cells occurs preferentially after a discrete number of cell divisions *in vivo*. *J Immunol* 1999; **162**: 6312–6315.
50 Boehme SA & Lenardo MJ. Propriocidal apoptosis of mature T lymphocytes occurs at S phase of the cell cycle. *Eur J Immunol* 1993; **23**: 1552–1560.
51 Russell JH, White CL, Loh DY & Meleedy-Rey P. Receptor-stimulated death pathway is opened by antigen in mature T cells. *Proc Natl Acad Sci USA* 1991; **88**: 2151–2155.
52 Green DR, Droin N & Pinkoski M. Activation-induced cell death in T cells. *Immunol Rev* 2003; **193**: 70–81.
53 Budd RC. Activation-induced cell death. *Curr Opin Immunol* 2001; **13**: 356–362.
54 Hirata H, Takahashi A, Kobayashi S, *et al*. Caspases are activated in a branched protease cascade and control distinct downstream processes in Fas-induced apoptosis. *J Exp Med* 1998; **187**: 587–600.
55 Inaba M, Kurasawa K, Mamura M, Kumano K, Saito Y & Iwamoto I. Primed T cells are more resistant to Fas-mediated activation-induced cell death than naive T cells. *J Immunol* 1999; **163**: 1315.
56 Adams JM & Cory S. The Bcl-2 protein family: arbiters of cell survival. *Science* 1998; **281**: 1322–1326.
57 Antonsson B & Martinou JC. The Bcl-2 protein family. *Exp Cell Res* 2000; **256**: 50–57.
58 St Clair EG, Anderson SJ & Oltvai ZN. Bcl-2 counters apoptosis by Bax heterodimerization-dependent and – independent mechanisms in the T-cell lineage. *J Biol Chem* 1997; **272**: 29347–29355.
59 Gross A, McDonnell JM & Korsmeyer SJ. Bcl-2 family members and the mitochondria in apoptosis. *Genes Dev* 1999; **13**: 1899–1911.
60 Guha M, Kumar S, Choubey V, Maity P & Bandyopadhyay U. Apoptosis in liver during malaria: role of oxidative stress and implication of mitochondrial pathway. regulation by extracellular signals: mechanisms and specificity. *FASEB J* 2006; **20**: 1224–1226.